A Comprehensive Study on Protection System Design for Doubly-Fed Induction Generator Wind Turbines under Voltage Sags

*Meliksah Ozakturk
*Faculty of Technology, Department of Energy Systems Engineering, Mustafa Kemal University, Hatay, Turkey

Abstract

A rotor crowbar (over-current protection) circuit with its improved control algorithm is designed in order to protect the rotor-side converter and the power electronic components of the doubly-fed induction generator (DFIG) wind turbine systems from the high rotor currents occurring in the rotor due to the voltage sags or grid faults. A DC-link brake (over-voltage protection) is also proposed to prevent the overcharging of the DC-link capacitor placed between the rotor-side converter and the grid-side converter. To investigate the behaviour and fault ride through performance of the DFIG system under the fault condition, a balanced three-phase voltage sag for different sag durations is applied to the network voltage in the simulation programme of PSCAD. Thus, the proposed protection schemes have been shown to work reasonably.

Key words: Doubly-fed induction generator, crowbar protection, DC-link brake, voltage sag, wind turbine.

1. Introduction

The protection of electronic devices used in the structure of power electronic converters is significant in order to protect the overall DFIG wind turbine system from the damaging effects of over-voltage and/or over-current phenomena. These typically occur in the system during the transient process , during and after the voltage sags or grid faults. Protection designs allow the cost of replacing the semiconductor devices to be avoided. In most DFIG-based wind turbines, a rotor crowbar circuit is used as an over-current protection while a DC-link brake is utilised for over-voltage protection.

Grid fault ride through techniques for wind turbines employing DFIGs are widely investigated to eliminate the harmful impacts of higher voltages and currents to the system in [1, 2-18]. In [2], the performance analysis of a DFIG under network disturbances is carried out by using a passive crowbar consisting of a three-phase diode bridge and a thyristor in series with a resistor. [3, 5, 13] investigate the ride through of DFIG-based wind turbines during a voltage sag. [13] uses a protection scheme of two anti-parallel thyristors with a series bypass resistors per phase, [5] implements that of inductor based fault emulator, and [1, 6-7, 9-14, 16-18] utilise that of a crowbar circuit. As seen from the references aforementioned, the most dominant protection method against over current is the rotor crowbar circuit.

The advanced crowbar protection configuration amongst variety of the crowbar options is one which consists of a diode bridge (rectifier), a rotor crowbar resistance and series insulated-gate bipolar transistor (IGBT) switch. Besides the rotor crowbar circuit, an additional protection

*Corresponding author: Address: Faculty of Technology, Department of Energy Systems Engineering, Mustafa Kemal University, 31600, Hatay, TURKEY. E-mail address: ozakturk@mku.edu.tr, Phone: +903267648888 Fax: +903267648866

scheme to prevent the DC-link capacitor overcharging is inserted between the rotor-side converter and grid-side converter, which is known as DC-link brake method. Another important function of the DC-link brake is to help the grid-side converter keep the DC-link voltage constant at a predefined value.

In this paper, the control algorithm of the rotor crowbar protection is further improved with a detailed presentation of logic circuit. Thus, enhanced protection control for the rotor crowbar circuit is maintained. With the insertion of the rotor crowbar protection, the sensitive power electronics devices are protected from the high currents occurring during the network faults. Optimum voltage threshold values for the DC-link brake control are determined as well.

2. Doubly-fed induction generator (DFIG) modelling

The main components of a typical DFIG wind turbine are back-to-back converters, i.e. a rotor-side converter and a grid-side converter, a DC-link capacitor placed between these two converters, and protection of power electronic components, e.g. a rotor crowbar circuit and a DC-link brake (see Figure 1). As seen in Figure 1, the DFIG is connected to the grid via a transformer while its rotor windings are connected to the rotor-side converter via slip rings.

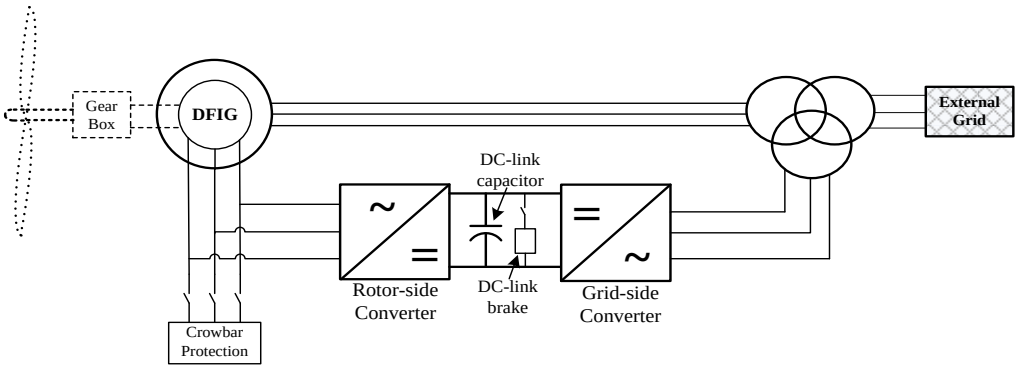

Figure 1: Typical DFIG wind turbine system

The rotor-side converter (RSC) controls the real and reactive power of the DFIG and provides the required magnetisation power to the generator through the rotor circuit. The grid-side converter (GSC) keeps the DC-link voltage constant at a preset value, which is maintained by a DC-link capacitor, and conveys the rotor power to/from the external grid. The control designs for the RSC and GSC have been documented in [19-21].

3. Protection system design

The designs of the rotor crowbar protection against over-current and the DC-link brake against over-voltage will be elaborated in the following sub-sections.

3.1. Rotor crowbar protection

The function of the (rotor) crowbar is to short-circuit the rotor through a resistance if the rotor

currents exceed threshold values. Once the crowbar protection is activated, the IGBTs of the rotor-side converter are all switched off and integrators of the controllers (e.g. power-outer loop controllers of the RSC) are reset to zero, i.e. the rotor blocks. Consequently, the DFIG system behaves as a squirrel-cage induction generator with a high resistance including additional rotor resistors.

The typical crowbar arrangements are shown in Figure 2. The crowbar circuit can be designed by placing two pairs of anti-parallel thyristors per phase connected to the rotor terminals (see Figure 2.a) or by using a combination of a diode bridge (rectifier) including a single thyristor and a rotor crowbar resistance, R_{cb}, (see Figure 2.b) [22]. The crowbar configurations seen in Figure 2.a and Figure 2.b are unable to quickly stop the rotor transient currents limiting the rotor-side converter restarting process. This is considered undesirable from the point of view of the fault ride-through technique [23]. An active crowbar shown in Figure 2.c is proposed in [1, 22] to resolve this issue. In an active crowbar arrangement, the rotor current can be stopped by using a forced commutation of the GTO-thyristor or an IGBT [23]. In this paper, the crowbar circuit depicted in Figure 2.c is used as a rotor crowbar protection of the DFIG-based wind turbine system.

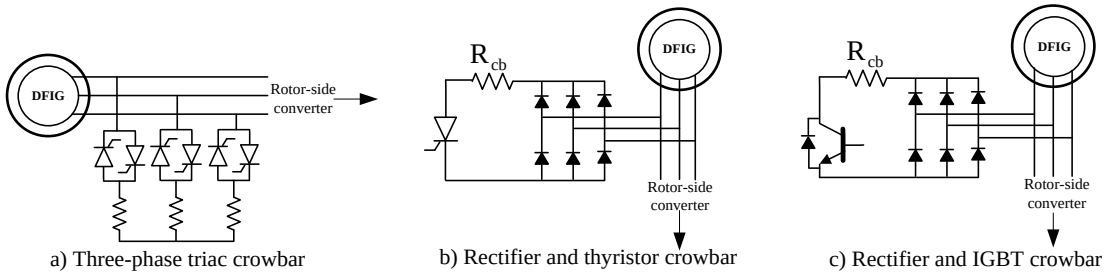

Figure 2: Typical rotor crowbar configurations

In [1, 24], the crowbar is activated if the rotor current exceeds 2pu while this threshold limit is taken down to 1.8pu in [25]. The authors in [26-28] propose the crowbar limit as 1.5pu. The threshold values for the rotor crowbar protection are defined as below:

$$i_{r\_a} \text{ or } i_{r\_b} \text{ or } i_{r\_c} > 2\text{pu} \quad \rightarrow \quad \text{Crowbar ON}$$
$$i_{r\_a} \text{ and } i_{r\_b} \text{ and } i_{r\_c} < 1.9\text{pu} \quad \rightarrow \quad \text{Crowbar OFF}$$

Thus an over-current occurring in any phase of the rotor current triggers the crowbar. Hysteresis is added and all three-phase currents together must be less than a lower threshold for the crowbar to be deactivated. In addition, a lock out time can be added to the control algorithm which allows the crowbar to stay ON (activated) for a reasonable time. This is maintained by a mono-stable block shown in Figure 3. The mono-stable block is used in order to delay the switch-off signal for a reasonable duration of time. By using this device, once the crowbar triggers it is expected that the crowbar stays switched-on for a fixed time and does not take further switch-on and -off actions. However, if the rotor currents persist exceeding the threshold value, the crowbar can switch on again until the over-current disappears. Nevertheless, reducing the switch-on and -off actions of the crowbar can help the whole system become less oscillatory and the switching

losses occurring in the system may then be diminished.

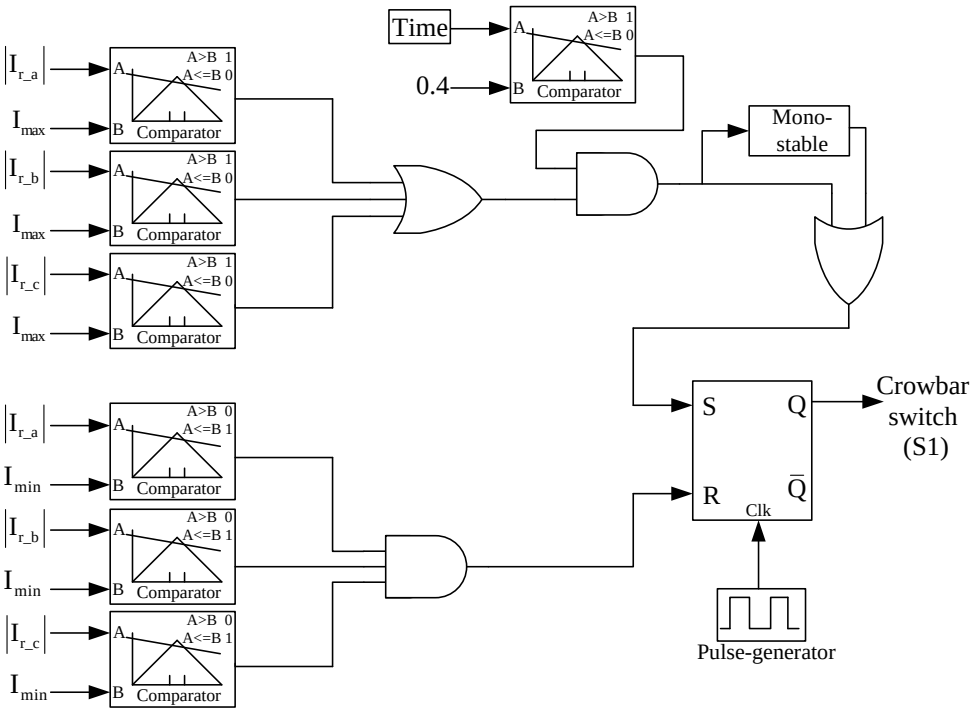

Figure 3: The control algorithm of the rotor crowbar protection scheme

Moreover, in order to prevent both the rotor crowbar protection and the DC-link brake from being activated at start-up, a time block may be added to their control algorithms and causes delay in activation of these protection devices for a desired duration from the beginning of the simulation. Therefore, start-up transients inherently existing in the system do not trip protection scheme in error. The control algorithm of the crowbar is depicted in Figure 3.

A typical fault ride through technique consists of these sequences: fault occurrence (or introducing voltage sag), triggering over-voltage (DC-link brake) and/or over-current protection (crowbar) switch, turning converter off, riding through fault, deactivating the protection and resuming the converter operation, maintaining synchronisation and finally returning to normal operation [23]. This operation needs integration into the rest of the system including the control.

3.2. DC - link brake method

A DC-link brake circuit, which is shown in Figure 4, is used to prevent the overcharging of the DC-link capacitor. The DC-link voltage is monitored and if it exceeds a certain threshold then the DC-link brake is activated.

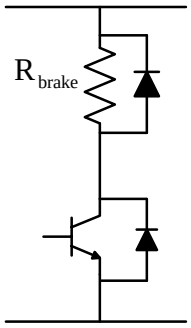

Figure 4: DC-link brake circuit

The maximum limit for overvoltage (DC-link) protection is set to 1.5pu in [24, 26]. There can be a risk of exceeding relay settings by over-current in the rotor circuit and by over-voltage in the DC-link when voltage drops down to 0.5pu or below [29]. In this paper, the DC-link brake is activated if the DC-link voltage (V_{DC}) exceeds 1.3pu of its nominal value, and if it is equal or less than 1.1pu, then the DC-link brake is deactivated. The control block diagram of the DC-link brake is shown in Figure 5.

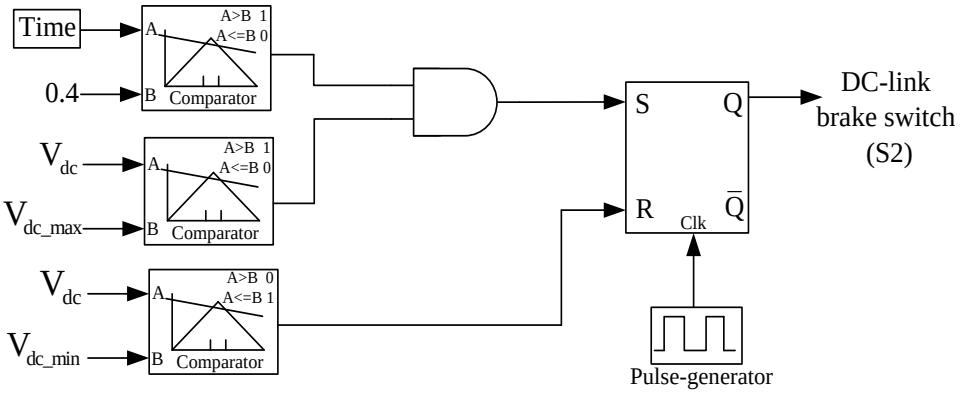

Figure 5: DC-link brake control design

4. Simulation Results

The fault ride through requirements for the majority of grid codes are elaborated in [30, 31]. The summary of ride through capability for wind turbine systems in different national grid codes is given as table in [31]. According to this table, the greatest fault duration is 625ms in US and Ireland while the lowest fault duration is designated as 100ms in Denmark. The simulation file of the DFIG system model depicted in Figure 6 is run with a fixed over-synchronous speed (generating mode) of 1.05pu. Since the three-phase fault condition is regarded as the worst case from the point of protection view, only the magnitude of 0.8pu three-phase voltage sag for the sag durations of 100ms, 250ms and 500ms is implemented at t=2s in order to meet the most national grid codes. The preset values of the stator real power (P_{s_set}), the stator reactive power (Q_{s_set}), the DC-link voltage and the three-phase network voltage are defined as 4.5MW (rated power), 0MVAr, 1kV and 33kV line-to-line RMS, respectively.

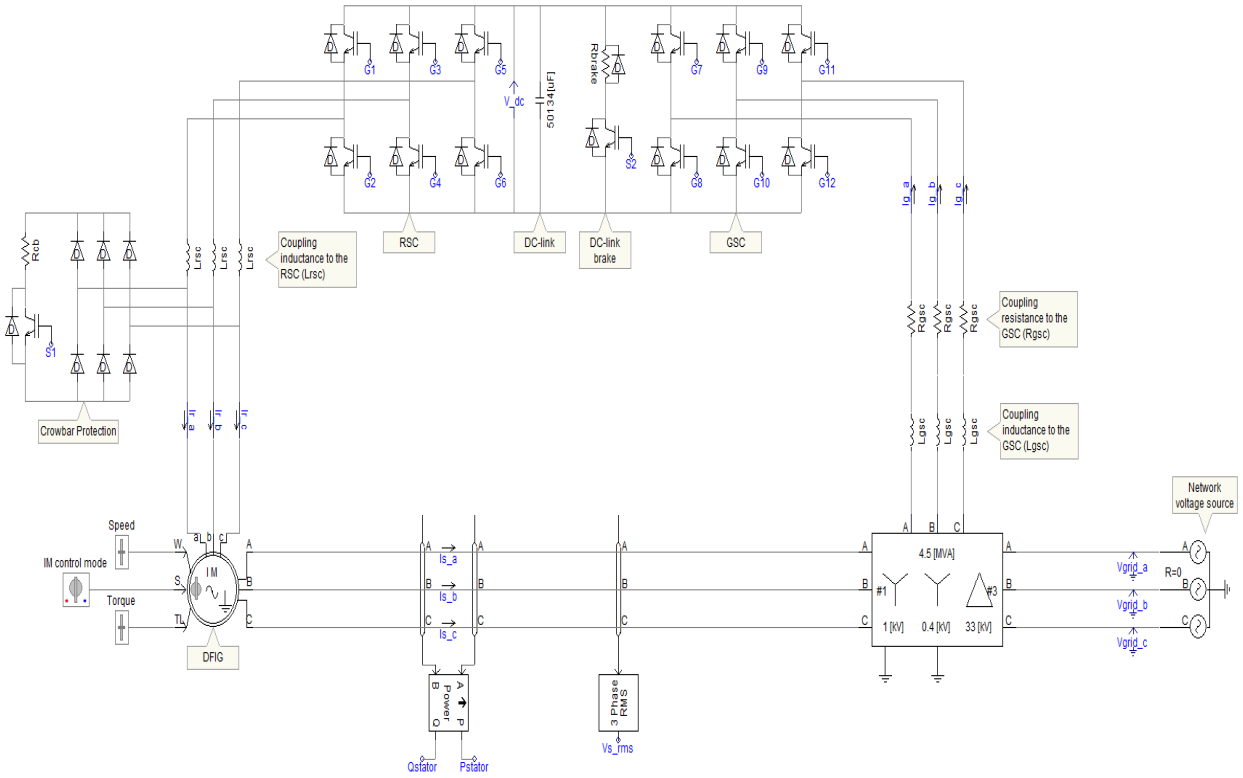

Figure 6: The DFIG system circuit in PSCAD

A severe three-phase voltage sag magnitude of 0.8pu is applied to the grid voltage source for a duration of 100ms and the relevant simulation results are illustrated in Figure 7. After the crowbar is deactivated, the stator active and reactive powers reach back to the steady-state in approximately 20ms but including the oscillations because the RSC resumes with causing just as the start-up transients, and due to the smoothing time constants of the power meters. The V_{DC} excursion is small enough and slow enough that the GSC outer (voltage) loop can pull the DC-link voltage back to its nominal value. There is only 10% oscillation occurs in the DC-link voltage until the steady-state condition. During the voltage sag or crowbar activation the q-component of the rotor voltage, which is proportional to the q-component of the rotor current and hence to the stator real power, fluctuates more than its q-component do. As seen in Figure 7, the protection system design introduced in this paper meets the grid code of Denmark which allows only 100ms fault duration with 1s recovery time [31].

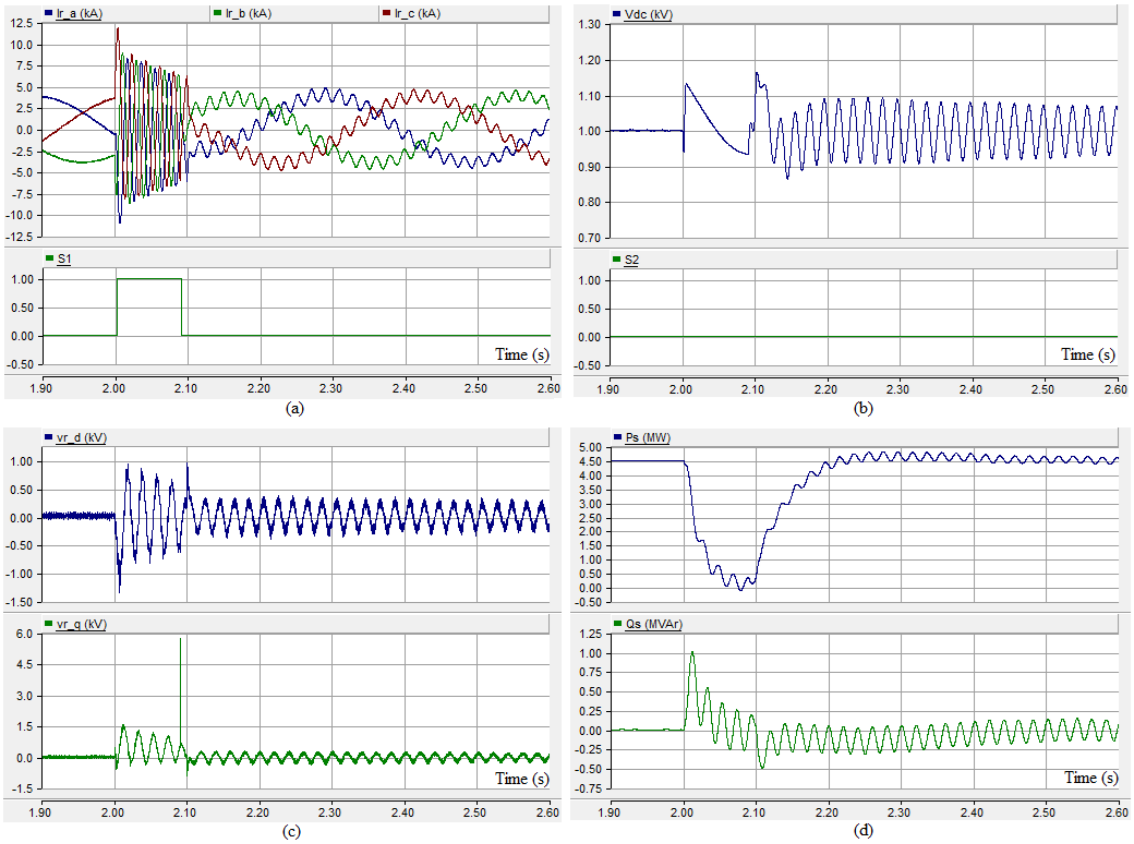

Figure 7: 0.8pu three-phase voltage sag application for a duration of 100ms
(a) Upper: The rotor currents in *abc* frame, Lower: The state of the crowbar switch
(b) Upper: The DC-link voltage, Lower: The DC-link brake switch
(c) Upper: The d-component of the rotor voltage, Lower: The q-component of the rotor voltage
(d) Upper: The stator real power, Lower: The stator reactive power

The same voltage sag is now applied for 250ms in order to verify whether the protection scheme can meet the Germany and UK national grid codes, and the results are demonstrated in Figure 8. Since the voltage sag duration is increased, the fluctuations in all output graphs increased too. The oscillations diminish right after the crowbar deactivation and the system reaches the steady-state. At approximately 2.26s, the stator real power meter indicates -1.5MW which means the DFIG starts to operate as motor for about 0.1s. The stator reactive power hits below -4.5MVAr meaning that the machine draws the reactive power from the grid from 2.26s to 2.7s, but this reactive power can be supplied by huge capacitor banks during the voltage sag. However, both the stator real and reactive power get back to steady-state in about 0.7s which is lower than the recovery times of Germany and UK grid codes. In comparison to those graphs shown in Figure 7, all output curves in Figure 8 have fewer oscillations when the crowbar deactivates and during the steady-state. The smoother DC-link voltage characteristic is also observed.

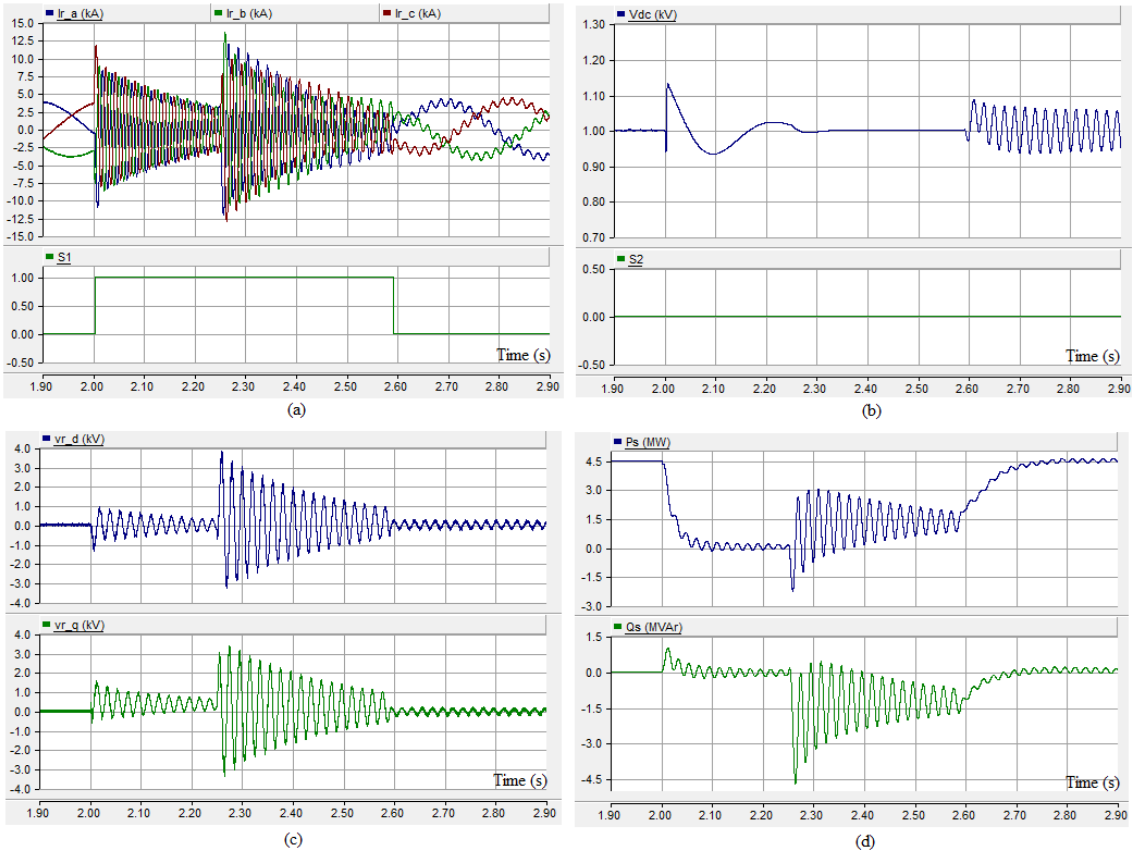

Figure 8: 0.8pu three-phase voltage sag application for a duration of 250ms
(a) Upper: The rotor currents in *abc* frame, Lower: The state of the crowbar switch
(b) Upper: The DC-link voltage, Lower: The DC-link brake switch
(c) Upper: The d-component of the rotor voltage, Lower: The q-component of the rotor voltage
(d) Upper: The stator real power, Lower: The stator reactive power

Finally, the same voltage sag is applied for 500ms and the simulation outputs are presented in Figure 9. The characteristics of these graphs seem to be effectively same as those in Figure 8 but with fewer oscillations. However, since the duration of the voltage sag doubles, the recovery time increases to approximately 1.2s. Thus, the grid codes of Ireland and USA are met. In addition, the recovery time of 1.2s of the proposed system is just 0.2s greater than that of the grid code requirement of Spain.

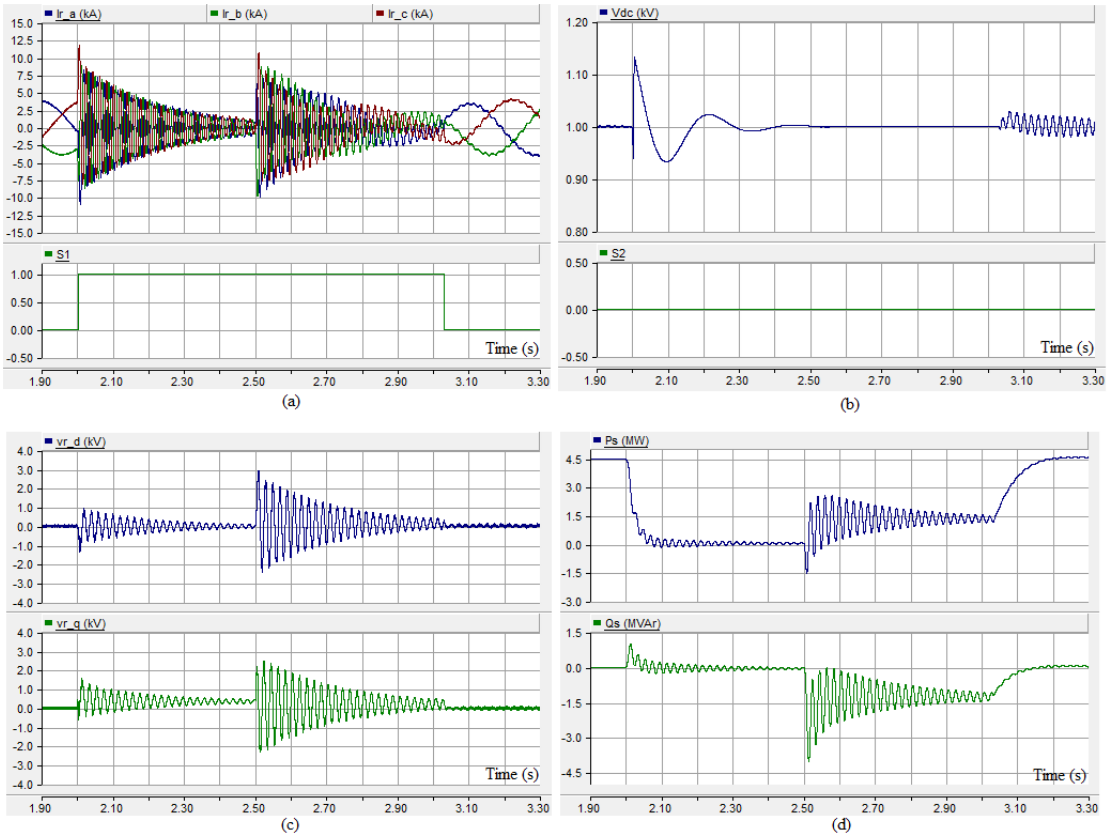

Figure 9: 0.8pu three-phase voltage sag application for a duration of 500ms
(a) Upper: The rotor currents in *abc* frame, Lower: The state of the crowbar switch
(b) Upper: The DC-link voltage, Lower: The DC-link brake switch
(c) Upper: The d-component of the rotor voltage, Lower: The q-component of the rotor voltage
(d) Upper: The stator real power, Lower: The stator reactive power

Conclusions

The circuits of the rotor crowbar protection and DC-link brake are designed. The controller algorithms of these protection schemes are shown to work sufficiently enough by applying the magnitude of 0.8pu three-phase voltage sag for the sag durations of 100ms, 250ms and 500ms is applied to the network voltage source. The results are examined as to whether some countries' grid code requirements are met. The interaction between the DFIG operational control, voltage sag behaviour, the DC-link brake and the rotor crowbar is investigated as well.

Due to the complexity of the system, the fluctuations occur in the outputs of the rotor currents, DC-link voltage, and stator active and reactive power during the introduction of the voltage sag. The oscillations diminish right away from the clearance of the voltage sag and will disappear once the system reaches again the steady-state.

References

[1] Pannell G. Grid fault ride through for wind turbine doubly-fed induction generators. EngD Thesis, Newcastle University, Newcastle, UK, 2008.
[2] Seman S, Niiranen J, Kanerva S, Arkkio A, Saitz J. Performance study of a doubly fed wind-power induction generator under network disturbances. IEEE T Energy Conver 2006; 21: 883-890.
[3] Morren J, de Haan SWH. Ridethrough of wind turbines with doubly-fed induction generator during a voltage dip. IEEE T Energy Conver 2005; 20: 435-441.
[4] Dawei X, Li R, Tavner PJ, Yang S. Control of a doubly fed induction generator in a wind turbine during grid fault ride-through. IEEE T Energy Conver 2006; 21: 652-662.
[5] Niiranen J. Experiences on voltage dip ride through factory testing of synchronous and doubly fed generator drives. In: 11th European Conference on Power Electronics and Applications; September 2005; Dresden, Germany.
[6] Seman S, Niiranen J, Arkkio A. Ride-through analysis of doubly fed induction wind-power generator under unsymmetrical network disturbance. IEEE T Power Syst 2006; 21: 1782-1789.
[7] Naess BI, Eek J, Undeland TM, Gjengedal T. Ride through solutions for doubly fed induction generators. In: 4th World Wind Energy Conference & Renewable Energy Exhibition; 2005; Australia.
[8] Holdsworth L, Charalambous I, Ekanayake JB, Jenkins N. Power system fault ride through capabilities of induction generator based wind turbines. Wind Engineering 2004; 28: 399-412.
[9] Foster S, Xu L, Fox B. Behaviour and protection of doubly-fed induction generators during network faults. In: IEEE Power & Energy Society General Meeting; 2009; Calgary, AB.
[10] Foster S, Xu L, Fox B. Coordinated reactive power control for facilitating fault ride through of doubly fed induction generator- and fixed speed induction generator-based wind farms. IET Renew Power Gen 2010; 4: 128-138.
[11] Anaya-Lara O, Wu X, Cartwright P, Ekanayake JB, Jenkins N. Performance of doubly fed induction generator (DFIG) during network faults. Wind Engineering 2005; 29: 49-66.
[12] Pannell G, Atkinson D, Kemsley R, Holdsworth L, Taylor P, Moja O. DFIG control performance under fault conditions for offshore wind applications. In: 18th International Conference and Exhibition on Electricity Distribution; 2005; Italy.
[13] Rodriguez M, Abad G, Sarasola I, Gilabert A. Crowbar control algorithms for doubly fed induction generator during voltage dips. In: 11th European Conference on Power Electronics and Applications; September 2005; Dresden, Germany.
[14] Erlich I, Wrede H, Feltes C. Dynamic behaviour of DFIG-based wind turbines during grid faults. In: Power Conversion Conference; 2007; Nagoya.
[15] Zhan C, Barker CD. Fault ride-through capability investigation of a doubly-fed induction generator with an additional series-connected voltage source converter. In: 8th IEE International Conference on AC and DC Power Transmission; 2006.
[16] Hansen AD, Michalke G. Fault ride-through capability of DFIG wind turbines. Renew Energ 2007; 32: 1594-1610.
[17] Pannell G, Atkinson DJ, Zahawi B. Analytical study of grid-fault response of wind turbine doubly fed induction generator. IEEE T Energy Conver 2010; 25: 1081-1091.
[18] Pannell G, Atkinson DJ, Zahawi B. Minimum-threshold crowbar for a fault-ride-through grid-code-compliant DFIG wind turbine. IEEE T Energy Conver 2010; 25: 750-759.

[19] Ozakturk M. Modelling and control system design for doubly-fed induction generator based wind turbines. In: 1st International Symposium on Innovative Technologies for Engineering and Science; 7-9 June 2013; Sakarya, Turkey, pp. 994-1003.
[20] Lei T, Barnes M, Ozakturk M. DFIG wind turbine modelling for detailed electro-magnetic system studies. IET Renew Power Gen 2013; 7: 180-189
[21] Lei T, Barnes M, Ozakturk M. Modelling and analysis of DFIG wind turbine system in PSCAD/EMTDC. In: 6th IET International Conference on Power Electronics, Machines and Drives; 27-29 March 2012; Bristol, UK.
[22] Niiranen J. Voltage dip ride through of a doubly-fed generator equipped with an active crowbar. In: Proceedings of Nordic Wind Power Conference; 2004.
[23] Perdana A. Dynamic models of wind turbines - A contribution towards to establishment of standardised models of wind turbines for power system stability studies. PhD Thesis, Chalmers University of Technology, Gothenburg, Sweden, 2008.
[24] Kayikci M. The influence of wind plant control on transient performance of the network. PhD Thesis, University of Manchester, Manchester, UK, 2007.
[25] Koch F, Shewarega F, Erlich I. Alternative models of the doubly-fed induction machine of power system dynamic analysis. In: International Conference on New and Renewable Energy Technologies for Sustainable Development; 2004; Evora, Portugal.
[26] Sun T, Chen Z, Blaabjerg F. Voltage recovery of grid-connected wind turbines with DFIG after a short-circuit fault. In: Power Electronics Specialists Conference; 2004.
[27] Zhou P, He Y. Control strategy of an active crowbar for DFIG wind turbine under grid voltage dips. In: Proceedings of International Conference on Electrical Machines and Systems; 2007; Seoul, Korea.
[28] Zhou P, He Y, Sun D, Zhu JG. Control and protection of a DFIG-based wind
[29] Akhmatov V. Analysis of dynamic behaviour of electrical power systems with large amount of wind power. PhD Thesis, Technical University of Denmark, Denmark, 2003.
[30] Tsili M and Papathanassiou S. A review of grid code technical requirements for wind farms.IET Renew Power Gen 2009; 3: 308-332.
[31] Iov F, Hansen AD, Sørensen P and Cutululis NA. Mapping of grid faults and grid codes.Risø-R-1617(EN), RISO, Denmark, July 2007.